Very low frequency phase advances during solar X-ray flares

Alessandra Abe Pacini[1,2], Jean-Pierre Raulin[1], Emília Correia[1,3], Pierre Kaufmann[1,4]

[1] CRAAM / Universidade Presbiteriana Mackenzie
[2] DGE / Instituto Nacional de Pesquisas Espaciais
[3] DAS / Instituto Nacional de Pesquisas Espaciais
[4] CCS / Universidade Estadual de Campinas

This paper was prepared for presentation at the 9th International Congress of the Brazilian Geophysical Society held in Salvador, Brazil, 11-14 September 2005.

Abstract

Very Low Frequency (VLF) waves propagate in the Earth-ionosphere waveguide bounded by the base of the D-region and by the ground. VLF waves are very sensitive to the electron density profile in the D region, and they can propagate over long distances keeping a high stability for the observed phase and amplitude parameters. For these reasons VLF waves provide a useful diagnostic of the low ionosphere, in terms of its parameters β (conductivity sharpness) and H (reflection height). This study reports on Sudden Phase Anomalies (SPA) of VLF waves received at Atibaia (São Paulo, Brazil) and at Inubo (Japan), from several long distance (over 2800 kilometers) paths during solar flares. The time coverage of the data sample includes periods of high solar activity (January-March 1991 and October-December 1991) as well as epochs of reduced solar activity (January 1994 - July 1997). This report allows us to investigate the detect ability of X-ray producing ionization excess in the low ionosphere, and how this situation is modified along the solar cycle. The results are also discussed in terms of solar flare properties like intensity and spectrum. In particular during solar minimum, we were able to identify a lower X-ray flux level needed to account for a SPA (~ 5.10^{-7} and 4.10^{-8} Wm^{-2} in the 1-8 Á and 0.5-4 Á energy ranges respectively). We also confirm the importance of the X-ray spectral characteristics for the properties of the observed SPAs.

Introduction

The physical processes acting in the region D of the ionosphere are poorly known, both because of the complex chemistry occurring there and of the sparse monitoring of this part of the ionosphere. Therefore temporal variations due to transient phenomena like solar flares, or on longer time scales during the solar cycle are still poorly understood in terms of the ionospheric parameters. The refractive index of the low ionosphere, for a propagating wave with frequency f= $\omega/2\pi$ in the VLF range, is governed by its electrical characteristics and depends on $\omega_p^2/\omega\nu$, where ω_p is the local plasma angular frequency and ν is the electron--neutral collision frequency. This dependency is obtained from the well-known Appleton-Hartree formula (Hargreaves 1992), neglecting magnetic field effects, and assuming $\nu >> \omega$ which is likely to be the case at the altitude of reflection of VLF waves (ν ~ few MHz). The above ratio is also written as ω_r/ω where ω_r is often called the conductivity parameter (Wait & Spies, 1964). Therefore, ω_r which depends on both the electron density and electron--neutral collision height profiles, is proportional to $e^{\beta(h-h0)}$, where h_0 is a reference height and β is the conductivity gradient (Wait & Spies, 1964). It is then common to define the ionospheric D region in terms of the 2 parameters, β (in km^{-1}), and the reflection height H (in km). During quiet solar condition, the X-ray emission from the Sun is probably not a significant source of ionization in the D region. However, at the time of explosive events on the solar disk, an excess of X-ray radiation hits the Earth and those photons with wavelength < 10 Á can penetrate down to D region altitudes or even lower, and change appreciably the parameters β and H there. In this paper we report sudden phase advances (SPA) detected on nine different long-range paths. In section 2 we present the instrumention used and describe the data analysis. Section 3 describes the detect ability of SPAs in the low ionosphere as a response to solar X-ray flares. In section 4 we study the dependence of SPAs with the solar zenith angle. Sections 5 and 6 report the comparison between SPAs and solar X-ray flares characteristics. In section 7 we present our concluding remarks.

2. Instrumentation and data analysis

SPAs have been monitored at Atibaia, São Paulo, Brazil, using VLF signals from the Omega navigation network transmitters, in both phase and amplitude. The tracking receivers were controlled by a Cesium beam atomic standard (Rizzo Piazza & Kaufmann 1975). Here we present phase measurements from North Dakota (NDAK), Haiku (HAI) and Argentina (ARG) transmitters, received at Atibaia (ATI) during the time periods 01/1991 - 03/1991, 10/1991 - 12/1991 (solar maximum), 01/1994 - 07/1997 (solar minimum). These data have been complemented by phase records received at Inubo (INU), Japan, during 10/1991 - 12/1991 at the time of SPAs (Ionospheric Data in Japan 1991), from transmitting stations located at La Reunion (LR), North West Cape (NWC), Liberia (L), NDAK, HAI and Australia (AUS). The comparison of SPA measurements and solar flare X-ray emission was done using the GOES full-disk detectors in the following energy channels: C1 (1 – 8 Δ) and C2 (0.5 - 4 Δ) corresponding to photons of energy between few keV and 15 keV. Flare starting and peak times have been measured to compare with the time evolution of the corresponding SPAs. A hardening factor, γ, has been estimated by the ratio of X-ray fluxes in the C2 and C1 channels. We have chosen SPA events during which each path was totally illuminated, or sunlit. Phase advances (in µs) have been transformed in degrees ($\Delta\phi$), and then normalized for the distance's path. For each event, and in order to discuss the effects of the solar zenith angle, χ, we have computed a mean value χ by averaging the χ computed for each 100 km of the total path. We have also considered the lower value of χ along the path, χ_{min}.

3. Detect Ability of Sudden Phase Anomalies

Among all the known Sudden Ionospheric Disturbances (SID) (Mitra 1974), SPAs are probably the most sensitive signatures of perturbations (Kaufmann et al. 1969). The minimum X-ray flux is a given wavelength range $F_{min\lambda}$, needed to produce a detectable SPA has been investigated in the past (Kreplin et al. 1962; Kaufmann et al. 1969; Muraoka et al. 1977; McRae et al. 2004). However, in most of these studies, SPAs are reported independently of the time period during which they occurred, i.-e. maximum or minimum of solar activity, and this could explain actually observed discrepancies between the $F_{min\lambda}$ values.

In Figure 1 we show a dispersion diagram for all the SPAs that have been associated with a solar flare detected in X-rays. The peak X-ray flux of each flare is shown in C1 (F_{c1} up) and C2 (F_{c2} bottom) photon energy ranges, as a function of the hardening factor and for different solar activity time periods (quiet: left plots; active: right plots). The horizontal dashed lines at $F_{\lambda 1} = 2 \,.\, 10^{-6}$ Wm^{-2} (top) and at $F_{\lambda 2} = 2 \,.\, 10^{-7}$ Wm^{-2} (bottom), allows us to see that during low solar activity time periods more than 30% of the C1 X-ray flares producing SPAs, have a peak flux lower than $F_{\lambda 1}$. A similar statement is also true for the C2 X-ray flares producing SPAs. These percentages fall down to less than a few percents during solar maximum epochs (right plots). At a first glance we could be tempted to conclude that the detect ability differences shown in Fig. 1 are due to a higher sensitivity of the ionosphere during solar minimum relative to that at solar maximum. However, the thick horizontal lines in Fig. 1 represent the minimum detectable flux, i.-e. the X-ray background , F_{bg}, which is much higher ($F_{bg} \sim 10^{-6}$ Wm^{-2} and $\sim 10^{-7}Wm^{-2}$ for C1 and C2 channels respectively) during solar maximum compared to solar minimum($F_{bg} \sim 5.10^{-8}$ Wm^{-2} and $\sim 5.10^{-9}$ Wm^{-2} for C1 and C2 channels respectively), due to the presence of many more X-ray emitting active centers on the solar disk. We note that during solar maximum the faintest solar events responsible for a SPA have a flux barely greater than F_{bg}. Such that $F_{min\lambda}$ cannot be determine at the time of high solar activity. On the other hand, during solar minimum we found that $F_{min\lambda}$ is well defined for both channels C1 and C2, with values of about 5.10^{-7} Wm^{-2} and 4.10^{-8} Wm^{-2} respectively, clearly above the corresponding backgrounds. We note that $F_{min} \sim 0{,}5.10^{-6}$ Wm^{-2} found for C1 during solar minimum, is well below any previous results in the same energy range. As said earlier, this is due the fact that the left plots in Fig. 1 only refers to solar events which occurred during solar minimum.

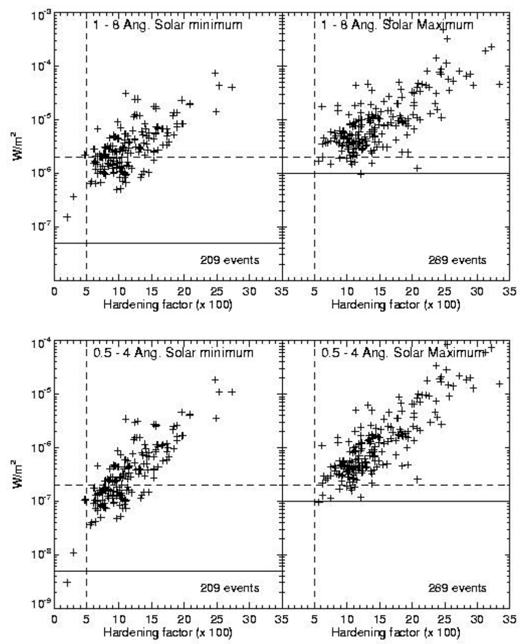

Figure 1 – Solar flare X-ray flux as a function of the hardening factor for events which produced SPAs during solar minimum (left) and solar maximum (right).

Finally Figure 1 informs us that the vast majority of the SPAs produced by solar flares have a hardening factor greater than 0.05, which then appears as a lower limit for the spectral shape of the solar flares producing SPAs, independently of the solar activity.

4. Dependence of Sudden Phase Advance on the Zenith angle χ

The amplitude of a SPA depends on the solar zenith angle, χ, at the time of the flare. This dependence has been studied by many authors (Chilton et al. 1963; Pant 1993). However, because of the difficulty of choosing a unique value for χ, and due to the fact that the χ dependence probably changes from flare to flare (Chilton, et al. 1963), the correction used is different from author to author. Kaufmann et al. (2002) consider only flares for which $\chi \leq 70°$, and Pant 1993 only corrects the SPA amplitude (by dividing by $\cos(\chi)$) for flares with $\chi \geq 81°$. Recently, McRae et al. (2004) have shown that the effect of a flare is not strongly dependent on its solar zenith angle, and thus do not correct the SPA amplitudes. In Figure 2 we show the result of the dependence on χ for nine events (numbered from 1 to 9 with increasing intensity in the C1 channel) which were well observed by at least three long range paths. For each event a mean solar zenith angle, χ_m, has been estimated and we plot Log[sec(χ_m)] versus Δh, where Δh is the change of upper waveguide height estimated from Wait & Spies (1964), assuming that the first order is the dominant mode of propagation. In order to compute Δh we have used the unperturbed height reference level given by McRae et al. 2004 as a function of χ, and which is valid for long range trans equatorial paths at middle and low latitudes. As found by (Chilton, et al. 1963), Figure 2 shows that for each flare it exits a relation between Log[sec(χ_m)] and Δh, although this relation is different from flare to flare. The abscissa where each line cuts the X axis would be the change of reflection height, $\Delta h_{\chi=0}$ for a zenith angle equals to zero. We note that for the larger solar flares the reflection height can be reduced as much as 14 km, reaching altitudes of ~ 56 km (for a reference level at 70 km).

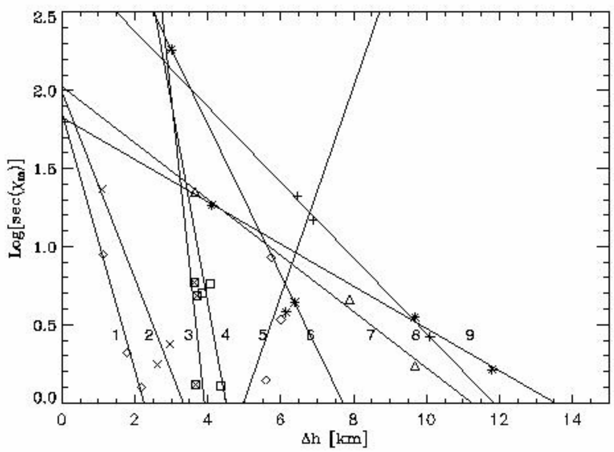

Figure 2 – Plot of Log[sec(χ_m)] as a function of the change in the reflection height Δh, for nine solar flares. Each SPA has been detected from at least tree different paths. Numbers 1 to 9 correspond to increasing values of F_{c1}.

In Figure 3 we have plotted, for the nine flares, $\Delta h_{\chi=0}$ versus F_{c1} (crosses) and F_{c2} (stars), and we note a high degree of linear correlation of about 0.91 and 0.88 respectively. Moreover, this figure shows that the dispersion generally observed in Δh (or $\Delta\phi$) versus F_{c1} and F_{c2} plots (see next section), which is due to the difficulty of finding at the time of a flare a unique value for χ (in particular for East-West oriented paths), is considerably reduced.

5. Dependence of Sudden Phase Advances on the solar flare characteristics

In Figure 4 we show the relation between the SPA amplitude and the peak of the corresponding solar flare,

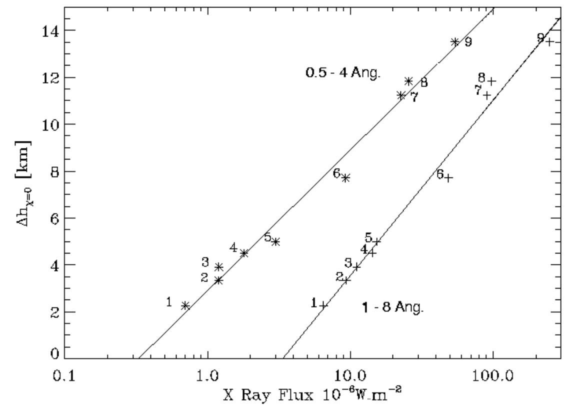

Figure 3 – Reflection height for χ = 0 for the nine flares of Fig. 2 versus F_{c1} and F_{c2}.

in both channels C1 and C2 and for periods of solar minimum (left plots) and solar maximum (right plots). The SPA amplitudes have been normalized for the distance of the paths. In addition, the amplitudes have been corrected for the sec(χ_{min}) factor, where, χ_{min} is the minimum value of the solar zenith angle along the path at the time of the flare. However, we mention that this last correction did not introduce great changes, since we have verified that the correlation shown in Fig. 4 is almost independent of the solar zenith angle, as found by McRae et al. (2004). Figure 4 leads to similar comments as those done for Fig. 1, in particular that the lower solar flux needed to produce a SPA is probably related to the X-ray flux background detected in channels C1 and C2, at least during solar maximum period (right plots).

However, Figure 4 also shows that it is difficult to reproduce the dispersion of the observed points using a single straight line. Instead, it seems that we can account for the data using different single straight lines, with slopes increasing with the X-ray peak flux. This is true during the solar minimum period (left), and also true, although to a lesser extent, for the solar maximum period. This property is shown in Figure 5, for channels C1 (top) and C2 (bottom), where we have distinguished those events with a hardening factor, $0.05 < \gamma \leq 0.1$ (left plots), $0.1 < \gamma \leq 0.15$ (middle plots), and $\gamma > 0.15$ (right plots). We note that a single straight line is able to adjust the observed points, independently whether the corresponding solar flares have been observed during solar minimum (crosses) or solar maximum (triangles). For both energy ranges, C1 and C2, the minimum peak fluxes needed to produce a SPA seems to increase with the hardening factor γ. This confirms the important role played by the spectrum of a given solar flare to understand the characteristics of the SPA it produced (Kaufmann et al. 1969).

Finally we note that the slopes of the fitting lines in Figure 5 increase with the factor γ, which simply indicates that the effective wavelength of the ionizing solar radiation decreases (Muraoka et al. 1977).

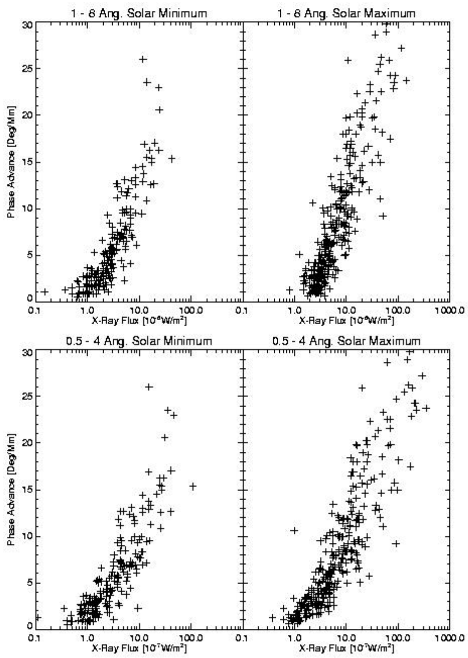

Figure 4 – Phase advances versus F_{c1} (top) and F_{c2} (bottom), during solar minimum (left) and solar maximum (right).

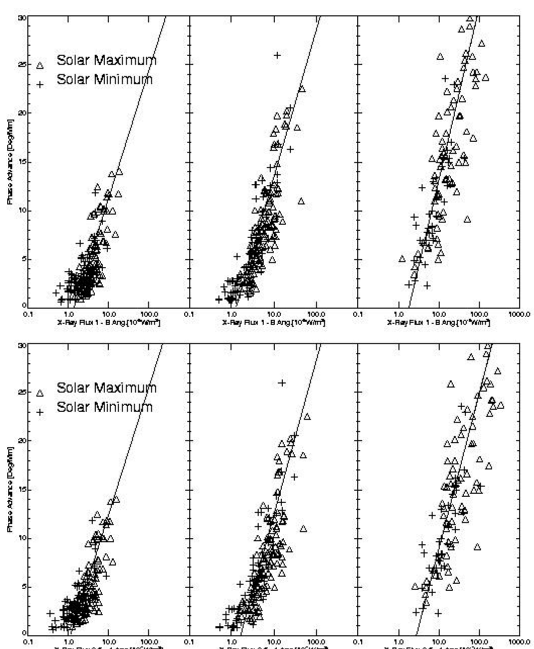

Figure 5 – Phase advances versus F_{c1} (top) and F_{c2} (botton). We fave grouped in the same plot solar flares occurring during solar minimum (crosses) and solar maximum (triangles). Left plots are for flares with $0.05 < \gamma \leq 0.1$, middle plots for $0.1 < \gamma \leq 0.15$ and right plots for $\gamma > 0.15$.

6. Temporal comparison between Sudden Phase Advances and flare evolution

We have studied also the delays (ΔT) observed between the maximum of a SPA and the peak time of the ionizing radiation which originated the ionospheric event. The results are shown in Figure 6 for four paths using the X-ray fluxes in channels C1 and C2. This figure shows that ΔT is about 3 minutes independently of the path. However, for the trajectory ATI-NDAK we found values greater by about a factor 2. This may have been due to the some instrumental effects of unknown origin.

We have found that the ΔT shown in Figure 6, are independent of the solar activity. We first note that there is a non negligible proportion of events for which $\Delta T \leq 0$. If we assume that the flare X-ray time profile represents the rate of ionization production at a given altitude, h, in the ionosphere, we should expect at this altitude the time profile of the electron density to have its maximum after the X-ray peak. The corresponding delay, also called relaxation time (Mitra 1974), should equals the observed ΔT. Therefore measurements with $\Delta T \leq 0$ are unlikely.

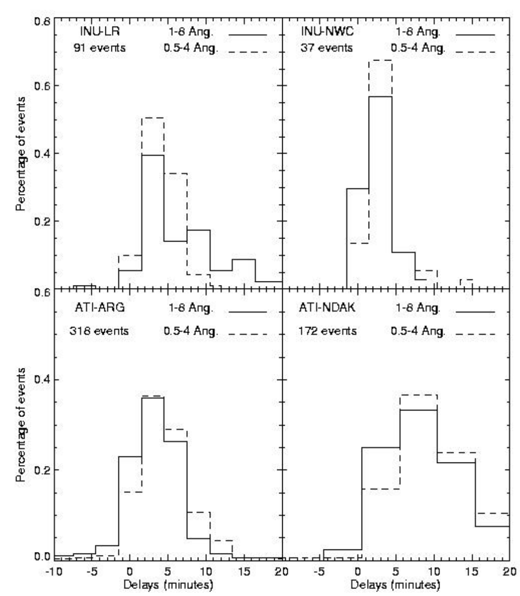

Figure 6 – Distribution of the delays (ΔT) between times of SPA and X-ray maxima, for four different paths. For the NDAK path, the time constant of the phase data is much higher (150 s) than for the other paths (50 s).

We stress the fact that among the observed flares, 22% show ∆T ≤ 0 using the C1 channel, while this percentage is only 14% for the same flares observed in the C2 channel, suggesting that the 0.5 – 4 ∆ photons are more efficient in producing SPAs. This again strengthens the fact that the harder the solar flare, the higher the probability it produces an ionospheric event (Kaufmann et al. 1969).

7. Concluding remarks

We have presented results about the detect ability of SPAs produced by increases of ionization in the low ionospheric D region during solar flares, as well as about the relation between SPAs properties and flare characteristics. We found that during solar minimum, it is possible to define a lower X-ray flux level to account for a SPA. This value is ~ 5.10^{-7} and 4.10^{-8} Wm^{-2} in the 1-8 ∆ and 0.5-4 ∆ energy ranges respectively. For solar maximum time periods, the background X-ray emission from all the emitting active centers in the solar disk, prevents to detect a lower threshold X-ray flux. By comparing the ionospheric response in the different X-ray energy ranges, we were able to confirm the importance of the X-ray spectral characteristics for the properties of the observed SPAs. In particular, and as reported in earlier works, we found that the harder the solar flare, the more important the ionospheric response. Such conclusion was also confirmed by the observed delays between SPAs and X-ray flare time maxima.

References

Chilton, C.J., Steele, F.K. & Norton, R.B. 1963, JGR, 68, 5421

Hargreaves, J.K. 1992, The solar-terrestrial environment, (Cambridge: Cambridge University Press)

Ionospheric Data in Japan 1991, vol. 43, Nos 10-12, Communications Research Laboratory. Ministry of Posts and Telecommunications, Tokyo, Japan

Kaufmann, P. & Paes de Barros, M.H. 1969, SolPhys., 9, 478

Kaufmann, P. Piazza, L.R. & Fernandez, J.H. 2002, JGR, 107, 30

Kreplin, R.W., Chubb, T.A. & Friedmann, H. 1962, JGR, 67, 2231

McRae, W.M. & Thomson, N.R. 2004, JATP, 66, 77

Mitra, A.P. 1974, Ionospheric effects of solar flares, (Dordrecht: Reidel)

Muraoka, Y., Murata, H. & Sato, T. 1977, JATP, 39, 787

Pant, P. 1993, Ap&SS, 209, 297

Rizzo Piazza, L. & Kaufmann, P. 1975, JATP, 37, 1281

Wait, J.R. & Spies, K. 1964, Natl. Bur. Std. Tech. Note, No 300